THE JOURNAL OF PHYSICAL CHEMISTRY Letters

Letter

pubs.acs.org/JPCL

Combining the Many-Body *GW* Formalism with Classical Polarizable Models: Insights on the Electronic Structure of Molecular Solids

Jing Li,[†] Gabriele D'Avino,[‡] Ivan Duchemin,[¶] David Beljonne,[‡] and Xavier Blase*[,†]

[†]Grenoble Alpes University, CNRS, Institut NÉEL, F-38042 Grenoble, France

[‡]Laboratory for Chemistry of Novel Materials, University of Mons, Place du Parc 20, BE-7000 Mons, Hainaut, Belgium

[¶]INAC, SP2M/L_Sim, CEA/UJF, Cedex 09, 38054 Grenoble, France

ABSTRACT: We present an original hybrid QM/MM scheme merging the many-body Green's function *GW* formalism with classical discrete polarizable models and its application to the paradigmatic case of a pentacene crystal. Our calculated transport gap is found to be in excellent agreement with reference periodic bulk *GW* calculations, together with properly parametrized classical microelectrostatic calculations, and with photoionization measurements at crystal surfaces. More importantly, we prove that the gap is insensitive to the partitioning of pentacene molecules in QM and MM subsystems, as a result of the mutual compensation of quantum and classical polarizabilities, clarifying the relation between polarization energy and delocalization. The proposed hybrid method offers a computationally attractive strategy to compute the full spectrum of charged excitations in complex molecular environments, accounting for both QM and MM contributions to the polarization energy, a crucial requirement in the limit of large QM subsystems.

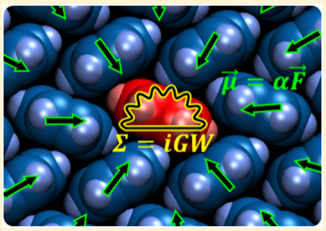

Hybrid quantum mechanics/molecular mechanics (QM/MM) approaches are invaluable tools for the theoretical study of complex supramolecular systems featuring disorder and heterogeneous chemical composition.[1,2] Organic semiconductors based on π-conjugated molecules or polymers belong to this category, standing as a severe challenge to the theoretical description of key properties such as charge-transport levels or optical excitations. The difficulty is twofold because, on one hand, one needs to rely on an accurate quantum mechanical description of the electronic structure and, on the other, the environment has to be properly taken into account. The latter is critical when dealing in particular with charged or charge-transfer excitations that experience strong reaction fields from the surrounding polarizable medium. In this context, QM/MM schemes offer an ideal compromise between accuracy and computational efficiency, and a few applications to organic semiconductors appeared in the last years, mostly based on density functional theory (DFT).[3−6]

Concerning the QM scheme, the *GW* many-body Green's function formalism[7−10] is a well-established technique in the computational physics community, where it brought considerable improvement over DFT in the calculation of the band structure of periodic systems by introducing proper nonlocal and state-dependent electronic correlations in an effective way. Such an approach is gaining increasing attention in the quantum chemistry community, thanks to efficient implementations based on Gaussian bases, allowing unbiased explicit comparisons with state-of-the-art wave function-based methods,[11−15] in complement to the earliest comparison with experiments,[16−33] for the electronic properties of gas-phase organic molecules. These studies showed the remarkable accuracy obtained at a computational cost that allows the study of systems comprising well above 100 atoms.[34−37] However, while *GW* calculations on periodic organic crystals have been recently performed,[38−41] the study of disordered systems is hampered by the lack of experience for the combination of the *GW* formalism with polarizable models,[35,42] calling for methodological developments accompanied by a clear validation as compared to reference techniques.

In this Letter, we report on the merging of the many-body *GW* formalism with accurate atomistic polarizable models based on first-principles inputs[43,44] and the application of this novel QM/MM approach to the study of the electronic properties of the prototypical molecular semiconductor pentacene. Besides validating the method against reference periodic *GW* calculations and experimental data, we will address the very fundamental issue of the partitioning of the system into QM and MM parts, emphasizing the crucial contribution of the QM subsystem to the polarization energy and demonstrating the need for a QM formalism that captures explicitly the electronic reorganization associated with charged excitations. Our conclusions allow one to clear previous misconceptions of the relationship between polarization and charge delocalization in organic solids.

Many-body perturbation theory provides a practical scheme for computing quasiparticle excitation energies, corresponding to the energy to add/remove one electron to/from a given QM system, as a perturbative correction to Kohn−Sham single-particle levels

$$E_n^{GW} = \varepsilon_n^{KS} + \langle \phi_n^{KS} | \Sigma^{GW}(E_n^{GW}) - V_{XC}^{DFT} | \phi_n^{KS} \rangle \quad (1)$$

Received: June 13, 2016
Accepted: July 7, 2016
Published: July 8, 2016

DOI: 10.1021/acs.jpclett.6b01302
J. Phys. Chem. Lett. 2016, 7, 2814−2820

Here, ε_n^{KS} and ϕ_n^{KS} are the eigenvalues and eigenfunctions of the starting DFT calculation (where n is the level index), obtained with a specific exchange−correlation potential V_{XC}^{DFT}, namely, the PBE0 functional[45,46] in the present study. $\Sigma^{GW}(E_n^{GW})$ is the self-energy operator, accounting for exchange and many-body nonlocal correlation effects, evaluated at the quasiparticle energy E_n^{GW}. Within the *GW* formalism, the self-energy is evaluated through Hedin's equations[7]

$$\Sigma(\mathbf{r}, \mathbf{r}'; E) = \frac{\mathrm{i}}{2\pi} \int \mathrm{d}\omega\, \mathrm{e}^{\mathrm{i}\omega 0^+} G(\mathbf{r}, \mathbf{r}'; E + \omega) W(\mathbf{r}, \mathbf{r}'; \omega) \tag{2}$$

$$G(\mathbf{r}, \mathbf{r}'; E) = \sum_n \frac{\phi_n(\mathbf{r})\phi_n^*(\mathbf{r}')}{E - \varepsilon_n + \mathrm{i}0^+ \times \mathrm{sgn}(\varepsilon_n - E_F)} \tag{3}$$

$$W(\mathbf{r}, \mathbf{r}'; \omega) = \nu(\mathbf{r}, \mathbf{r}') + \int \mathrm{d}\mathbf{r}_1\, \mathrm{d}\mathbf{r}_2\, \nu(\mathbf{r}, \mathbf{r}_1)\chi_0(\mathbf{r}_1, \mathbf{r}_2) W(\mathbf{r}_2, \mathbf{r}'; \omega) \tag{4}$$

$$\chi_0(\mathbf{r}, \mathbf{r}'; \omega) = \sum_{i,j} (f_i - f_j) \frac{\phi_i^*(\mathbf{r})\phi_j(\mathbf{r})\phi_j^*(\mathbf{r}')\phi_i(\mathbf{r}')}{\varepsilon_i - \varepsilon_j - \omega - \mathrm{i}0^+ \times \mathrm{sgn}(\varepsilon_i - \varepsilon_j)} \tag{5}$$

where G is the time-ordered one-body Green's function and χ_0 the independent-electron susceptibility, while ν and W are the bare and screened Coulomb potential, respectively. Calculating χ_0, G, and W using the input Kohn−Sham eigenstates leads to the so-called perturbative G_0W_0 scheme, while reinjecting the corrected eigenvalues and/or eigenstates allows one to perform self-consistent *GW* calculations, with variations on the order of a few tenths of an eV on the calculated pentacene quasiparticle energies, as detailed below.

The present QM/MM implementation relies on the neglect of wave function overlap between the QM subsystem, described at the *GW* level, and the much larger classical (MM) region. Under this assumption, eq 5 indicates that χ_0 does not couple the QM and MM subsystems. It can then be shown after some algebra[42] that one can restrict eqs 2−5 to the QM subsystem by replacing the bare Coulomb operator ν with $(\nu + \nu_{reac})$, where

$$\nu_{reac}(\mathbf{r}, \mathbf{r}') = \int \mathrm{d}\mathbf{r}_1\, \mathrm{d}\mathbf{r}_2\, \nu(\mathbf{r}, \mathbf{r}_1)\chi^{MM}(\mathbf{r}_1, \mathbf{r}_2)\nu(\mathbf{r}_2, \mathbf{r}') \tag{6}$$

is the reaction field generated in $\mathbf{r}'$ by the MM subsystem in response to a charge added to the QM region at position $\mathbf{r}$. We stress that the χ^{MM} response function is here the full (interacting) susceptibility of the MM system in the absence of the QM subsystem but accounts for the self-consistent coupling of the MM degrees of freedom. In practice, once ν_{reac} is known for a given system, the *GW* calculation for the embedded QM region is equivalent to a gas-phase *GW* calculation, except for the important difference that the bare Coulomb potential is dressed by the polarizability of the environment. We emphasize further that while we neglect the electronic overlap between the QM and MM systems, the electronic delocalization in the QM system, which can be composed of several molecules, is fully considered.

Equations 2−5 show that the construction of the *GW* self-energy requires the dynamically screened $W(\omega)$ Coulomb potential. The frequency dependence of the dielectric properties in the visible range is experimentally known for organic crystals as pentacene,[47] although classical discrete polarizable models usually target the optical dielectric response in the $\omega \to 0$ low-frequency limit.[44] While the generalization of MM polarizable models to dynamical response is certainly possible, here we adopt another strategy that consists of merging static polarizable models with the static limit of *GW*, the so-called static Coulomb-hole plus screened exchange (COHSEX) formalism.[7,48] Such an approach was proposed in recent studies of the renormalization of molecular energy levels close to a metallic substrate[49,50] and validated quantitatively in the case of the merging of the *GW* formalism with the continuous polarizable model (PCM)[42] by comparison with reference ΔSCF calculations at the DFT and CCSD levels combined with the same PCM model. In practice, we write the *GW* quasiparticle energies in the presence of the polarizable MM medium as follows

$$\begin{aligned} E_n^{GW/MM} &= E_n^{GW} + (E_n^{GW/MM} - E_n^{GW}) \\ &\simeq E_n^{GW} + (E_n^{COHSEX/MM} - E_n^{COHSEX}) \\ &= E_n^{GW} + \sigma_n P_n^{COHSEX/MM} \end{aligned} \tag{7}$$

where we introduced the MM contribution to the state-specific polarization energy computed at the COHSEX/MM level ($P_n^{COHSEX/MM}$), defined as a positive quantity ($\sigma_n = +1/-1$ for occupied/unoccupied levels). This formula approximates the *GW*/MM calculation by a full gas-phase *GW* calculation plus a polarization correction calculated at the static level, namely, as the difference between two COHSEX calculations including or not the reaction field (ν^{reac}) contribution. The reason for such a formulation is that the use of the COHSEX approximation in the form of a difference allows reduction of the error introduced by replacing the frequency-dependent dielectric function by its low-frequency limit.

Our QM calculations are based on the FIESTA package[11,20,51] that implements the *GW* formalism exploiting Gaussian bases and a contour-deformation approach to the calculation of the energy integral in eq 2. We hence do not evaluate the reaction field via eq 6 and focus instead on the matrix elements

$$\nu_{reac}(\beta, \beta') = \int \mathrm{d}\mathbf{r}\, \mathrm{d}\mathbf{r}'\, \beta(\mathbf{r})\nu_{reac}(\mathbf{r}, \mathbf{r}')\beta'(\mathbf{r}') \tag{8}$$

between auxiliary Gaussian orbitals[52] located on the atomic sites in the QM region. This auxiliary basis stems from the Coulomb-fitting resolution-of-the-identity (RI-V) formulation of the *GW* implementation that we adopt. Knowledge of the reaction field in the auxiliary basis allows calculation of the response to any perturbation in the QM part and, in particular, the polarization energy associated with charging any occupied/virtual energy level.

The elements of the reaction field matrix $\nu_{reac}(\beta,\beta')$ are obtained by computing the energy of a probe charge in an auxiliary function β' in the self-consistent reaction field of MM molecules polarized by a source charge in β. The MM subsystem can be described by any continuum[42] or discrete polarizable model. Here the focus is on atomistic polarizable models, and we mostly rely on the charge response (CR) model by Tsiper and Soos[53] as implemented in the MESCAL package,[44] which provides a very accurate description of the static dielectric response of molecular crystals,[54,55] as an improvement over the simpler induced dipole (microelectrostatic, ME) scheme.[44] Both models feature anisotropic molecular linear response and take as input the molecular

DOI: 10.1021/acs.jpclett.6b01302
J. Phys. Chem. Lett. 2016, 7, 2814−2820

polarizability tensor computed at the desired level of accuracy. The polarization energy in the bulk limit, or at the surface of a semi-infinite crystal, responsible for the ∼2 eV closing of the gap from the gas to the bulk phase, is obtained by extrapolating the reaction field matrix elements computed on (semi)spherical clusters of increasing radius (see Figure 1). We focus here on

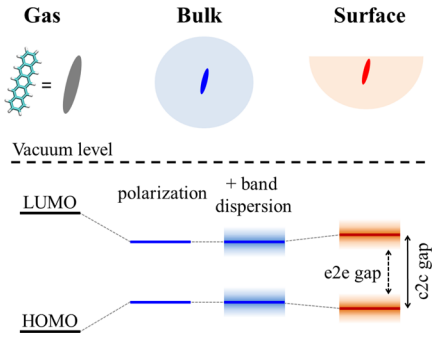

Figure 1. Illustration of the evolution of the frontier energy levels from the gas phase to the bulk crystal and surface in an organic semiconductor, assuming a common vacuum level. In the condensed phase, polarization effects reduce the gap by ∼2 eV, while dispersion broadens electronic bands. Transport levels at surfaces, as probed by photoelectron spectroscopies, differ from those in the bulk, resulting in general in larger gaps. The dashed arrow shows the band edge-to-edge (e2e) gap as usually defined in experiments, and the full arrow shows the band center-to-center (c2c) gap.

the polarization reaction to an added charge in the QM system, not considering the electrostatic interaction with the quadrupole field of the MM pentacenes[56−59] that has been shown to cancel almost exactly[56,60] in the total $P = P_H + P_L$ polarization contribution to the bulk gap value.

We start the presentation of our results focusing first on methodological aspects, discussing the impact on the electronic properties of the partitioning of the system into QM and MM subsystems. The arbitrariness of the choice of QM and MM subsystems is common to any hybrid scheme, and we aim at resolving this critical issue by comparing the gap for one or a few QM pentacene molecules embedded in an infinite pentacene MM crystal. Specifically, we consider QM clusters of one, three, and five neighboring pentacenes along the crystal axis $\vec{a}$ of the vapor-grown pentacene polymorph[61] that we study here; see Figure 2a−c. In light of the upcoming discussions, we selected that crystallographic direction as a test case because it exhibits large electronic overlap and delocalization for holes, electrons, and excitons. These three systems are rigorously identical in terms of geometry and differ by the exchange of molecules between the QM and MM subsystems.

The band gaps calculated for these three QM/MM systems are shown in Figure 2d. Because QM systems of more than one molecule feature the opening of HOMO and LUMO manifolds, the comparison focuses on the band center-to-center (c2c) gap (see Figure 1). We start with the PBE0 gas-phase data (blue bars, Figure 2d), showing, as expected, a too small 2.54 eV Kohn−Sham HOMO−LUMO gap as compared to the experimental 5.2 eV value.[62,63] Further, when increasing the number of pentacene molecules, one observes that the PBE0 c2c gap remains constant. Such a result is the signature that the use of Kohn−Sham energies does not allow one to capture the polarization effects at the origin of the large gap closing from the gas to the bulk phase (see Figure 1). Such results are consistent with previous PBE calculations[38,39]

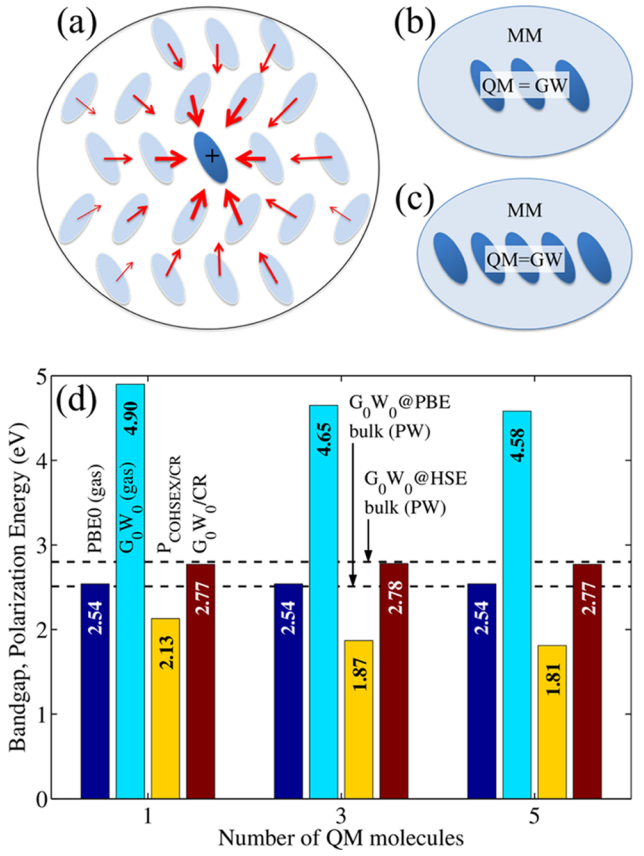

Figure 2. (a) Sketch of the QM/MM setup in the pentacene crystal with one QM molecule embedded in the polarizable MM environment. In (b) and (c), the QM part is expanded to three and five pentacenes. (d) Evolution of the HOMO−LUMO band center-to-center gap as a function of the size of the QM subsystem, computed for the QM system only (gas phase) at the PBE0 (blue bars) and G_0W_0@PBE0 level (cyan bars), as well as for the QM/MM system at the G_0W_0/CR level (brown bars). The polarization energies $P_{COHSEX/CR} = P_H + P_L$ are shown as yellow bars. The variations of the G_0W_0 molecular gap and P_{COHSEX} compensate for each other, leading to a QM size-independent gap. The horizontal lines mark the gap obtained with plane-wave G_0W_0@PBE (vapor polymorph)[38] and G_0W_0@HSE (solution polymorph)[39] calculations.

showing that gas and bulk Kohn−Sham c2c gaps are within 0.1−0.2 eV of each other.

The situation changes dramatically when adopting the *GW* formalism that explicitly deals with true charged excitations. As a first observation, performing a simple G_0W_0@PBE0 calculation, the gas-phase gap value is dramatically improved to 4.9 eV, in much better agreement with experiment.[62,63] Further, upon increasing the size of the QM subsystem, the gas-phase QM cluster c2c gap (cyan bars) is seen to decrease steadily when the number of pentacene molecules increases, in great contrast with the DFT Kohn−Sham case. This is the signature that polarization effects within the QM subsystem start closing the c2c gap. However, when considering now the bulk (embedded) G_0W_0@PBE0/CR gap (brown bars), accounting for the contribution of the MM reaction field to the screened Coulomb potential *W*, one observes that the bulk c2c gap (∼2.77 eV) is independent of the size of the QM subsystem. Such a gap stability stems from the reduction of the COHSEX/MM contribution to the polarization energy (yellow bars) that compensates exactly for the increase of the QM

DOI: 10.1021/acs.jpclett.6b01302
J. Phys. Chem. Lett. 2016, 7, 2814−2820

contribution to the polarization energy. This is a crucial result demonstrating that *the use of a QM/MM scheme that fully accounts for both QM and MM polarization effects permits one to vary the size of the QM subsystem without any loss in the polarization energy.* Such a behavior clearly stands as a strong requirement in the limit of large QM sections that are often needed when exploring molecular complexes with important hybridization or charge-transfer phenomena involving several molecules.

Our ∼2.8 eV *GW*/CR bulk c2c gap compares very well with the values from reference "full QM" *GW* calculations for periodic bulk systems reported in the literature, which display small variations stemming from different polymorphs and starting DFT functional. The G_0W_0@PBE calculations by Tiago et al. yielded a c2c gap of 2.51 and 2.67 eV for the vapor[61] and solution[64] grown polymorph,[61] respectively.[38] Sharifzadeh et al. applied G_0W_0@HSE to the solution polymorph, obtaining a gap of 2.8 eV,[39] while Kang et al. reported 2.89 eV for the SiO_2 thin-film structure[65] on the basis of partly self-consistent GW_0@PBE calculations.[40,66]

Our calculations are also sensitive to the starting DFT functional, or to the use of self-consistency,[66] that may affect the gap by a few tenths of an eV.[38−41] For example, performing a simple self-consistent scheme by reinjecting the corrected quasiparticle energies in the construction of *G* and *W* (see eqs 2−5), a scheme labeled ev*GW*, the gas-phase pentacene gap increases to 5.18 eV (cc-pVTZ value), in nearly perfect agreement with experiment. An important finding however is that the COHSEX/CR polarization energy that we calculate within our hybrid scheme is nearly independent of the starting DFT calculations and/or the use of self-consistency, with variations within 3% when, for example, changing from PBE0 to M06-2X[67] as the starting functional, namely, from 25 to 54% of exact exchange. As such, the accuracy of the gas-phase *GW* calculations will directly affect that of the bulk results.

We now compare the obtained polarization energies in the limit of a single QM pentacene molecule with the result of standard CR calculations. Table 1 provides such a comparison

Table 1. Polarization Energies (in eV) for the Hole (HOMO, P_H) and Electron (LUMO, P_L) Obtained with Hybrid COHSEX/CR and Standard CR Calculations for Pentacene Bulk and the (001) Surface[a]

	bulk		surface (001)	
	P_H	P_L	P_H	P_L
COHSEX/CR	1.00	1.12	0.91	1.02
CR	0.88	1.03	0.78	0.93

[a]The two approaches provide very similar results. Polarization energies are reduced by about ∼10% when going from the bulk to the vacuum interface.

for the bulk crystal and at its (001) surface, showing that the two approaches yield results that are within ∼10%. It is worth stressing, nevertheless, that the COHSEX/CR and CR results come from very different types of calculation. In the first case, polarization energies derive from the expectation values on Kohn−Sham eigenfunctions of the *GW* operator (eq 1) where the polarization of the environment enters the screened Coulomb potential *W* through the reaction field matrix $\nu_{reac}(\beta,\beta')$ (eqs 4 and 8). In standard ME or CR approaches, the polarization energy is instead computed as the difference in the extensive total energies of the system with and without the frozen charge of an ionized molecule in the QM subsystem.[44,53] Clearly, in the limit of a single QM molecule, the polarization energy originates mainly from the MM subsystem, keeping in mind however that only the COHSEX/CR approach accounts for the self-consistent coupling of the QM and MM susceptibilities.

The agreement of our *GW*-based QM/MM approach with reference *GW* results and established CR techniques provides the necessary validation steps, so that we are now in the position to compare our estimate for the pentacene gap with experimental results from ultraviolet photoelectron spectroscopy (UPS)[57] and low-energy inverse photoelectron spectroscopy (LEIPS).[59] These techniques are known to probe the first ∼2 nm below the surface, collecting thus mostly the signal from the topmost molecular layer. An advantage of our hybrid approach is that it can be used to study disordered and/or heterogeneous systems, as planned in our future work, or, as in this case, molecules at the surface of an otherwise three-dimensionally periodic solid, as shown in Figure 1.

The polarization energies and the gap of molecules on the (001) pentacene surface are reported in Tables 1 and 2,

Table 2. Computed (*GW*/CR) and Experimental Pentacene Transport Gap (in eV) Defined as the Band Center-to-Center[a]

	bulk	surface (001)
G_0W_0 + COHSEX/CR	2.77	2.96
ev*GW* + COHSEX/CR	3.05	3.25
experiment		3.4

[a]See Figure 1. The PBE0 functional has been used as a starting point for *GW* calculations. The self-consistent ev*GW* provides a gap of 5.18 eV for an isolated pentacene, yielding excellent agreement with gas-phase experimental data[62,63] and with measurements on films when surface embedding is accounted for in the calculation. Experimental data are taken from refs 57 and 59, with a typical uncertainty of 0.1 eV.

respectively. As expected, the polarization energies for molecules at the interface to vacuum are smaller than those in the bulk, leading to a ∼0.2 eV larger gap, as qualitatively illustrated in Figure 1. This increase of the gap at the surface is consistent with results from continuum[39] and atomistic polarizable models.[60,68] The calculated gap at the (001) surface (3.25 eV) is in excellent agreement with the experimental c2c gap value (∼3.4 eV; see Table 2) when using the self-consistent ev*GW* scheme that provides a very accurate gas-phase gap value. For the sake of completeness, we should mention that our frozen-nuclei calculations do not account for intramolecular structural relaxation upon ionization.[63]

The results discussed so far concern only ionization from/to the frontier orbitals HOMO and LUMO, although, as emphasized here above, once the reaction field matrix is obtained, the polarization energy associated with any other orbital of the system can be obtained. Notice that this is a unique feature of our hybrid method that results from the underlying *GW* formalim. Atomistic polarizable models,[44,53] DFT, or Hartree−Fock calculations for the gas-phase molecules or supramolecular systems[69,70] or other QM/MM schemes[3,4,6] can only access the first ionization potential and electron affinity as the energy difference between charged and neutral system (ΔSCF approach). For the sake of illustration, Figure 3 shows the polarization energy associated with a few occupied and unoccupied states in the bulk and at the (001) surface.

DOI: 10.1021/acs.jpclett.6b01302
J. Phys. Chem. Lett. 2016, 7, 2814−2820

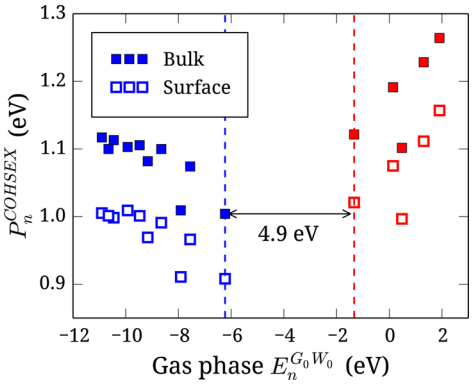

Figure 3. COHSEX/CR polarization energy (P_n in eq 7) for several pentacene occupied (blue) and unoccupied (red) states plotted against the gas-phase G_0W_0 level energy. The filled and empty squares correspond to ionization of a pentacene molecule in the bulk and at the (001) surface, respectively.

Clearly, the polarization energy is weakly state dependent among occupied (or unoccupied) states, with variations presumably related to the different spatial shape of the orbitals. The possibility of obtaining the polarization energy associated with all occupied/virtual energy levels opens the way to the calculation of the optical properties where the contribution from all transitions between electronic energy levels is required.

Before concluding, we discuss some general implications of our finding and clear up some misconceptions on the interplay of dielectric screening and charge delocalization. A large (0.2−0.5 eV) decrease of the polarization energy upon delocalizing a charge over several monomers of a polymer chain,[71] or molecules in a crystal lattice,[72] has been reported on the basis of microelectrostatic calculations, treating delocalized charges as supermolecules. These results are consistent with the decrease of the MM contribution to the polarization energy that we observe in the present scheme (yellow bars in Figure 2d). We emphasize again however that such a reduction, previously attributed to the delocalization of the added charge over several molecules, completely disappears upon the proper inclusion of the QM contribution to the polarization energy and thus cannot be taken as a truly physical phenomenon. The stability of the c2c gap in our QM/MM scheme upon increase of the QM subsystem is a clear necessary requirement that can only be fulfilled by selecting a QM scheme that fully includes polarization effects such as the *GW* formalism.

As another important consequence, the stability of the c2c gap as a function of the QM section size, namely, the stability of the total (MM + QM) polarization energy with respect to the delocalization of HOMO/LUMO manifold wave functions over several molecules, justifies the common assumption that dispersion effects, at the origin of the bandwidth in the solid state, can be straightforwardly added to the band center energies determined assuming localized carriers in a relaxed dielectric environment, as shown in Figure 1 (see also, e.g., ref 59), supporting further recent attempts to provide a multiscale description of the electronic structure of large complex supramolecular systems.[73,74]

In summary, we presented a novel hybrid QM/MM method merging many-body perturbation theory and atomistic polarizable models that we validated against reference calculations and experimental data. This approach, combining the merits of the *GW* formalism with an accurate description of the environment, represents a highly valuable tool for the study of charged states in complex molecular environments, such as organic semiconductors or biological systems. We demonstrated in particular the need for a QM scheme that fully captures polarization effects in order to ensure that the calculated QM/MM electronic properties are independent of the arbitrary partitioning between the QM and MM subsystems. This allows an increase of the size of the QM partition, fully accounting for all polarization contributions, while incorporating the proper description of charge transfer and hybridization between molecules in the QM region. Our results clarify the relation between polarization energy and charge delocalization, providing a rigorous framework for the treatment of dispersion effects in standard QM/MM approaches. Finally, our scheme provides polarization energy to all electronic energy levels, opening the way to optical calculations.

EXPERIMENTAL SECTION

The Kohn−Sham eigenstates needed to start the *GW* calculations are obtained with the NWChem[75] computational package at the PBE0/cc-pVTZ[76] level. Within the RI-V technique, we adopt the universal Weigend Coulomb fitting auxiliary basis.[52] The COHSEX/CR polarization energies are affected by less than 10 meV when adopting instead the 6-311G* principal basis and/or the cc-pVTZ-RI auxiliary basis.[77] In the limit of large systems, most of the CPU time is spent calculating the gas-phase *GW* quasiparticle energies, which typically vary from 2 to 18000 h from the 1-pentacene to the 5-pentacene QM system (calculations performed on Intel E5-2690 2.6 GHz cores). Even though presenting the same $O(N^4)$ scaling, the corresponding static COHSEX calculations take 0.16 and 622 h, respectively. Molecular polarizabilities of the MM part have been computed at the B3LYP/6-311++G** level, while the CR atom−atom polarizability tensor comes from INDO/S calculations.[53] Typical variations (≤10%) in polarization energies with respect to different choices of MM model and parametrization can be found in refs 44 and 78. The unit cell and atomic positions are the experimental ones as provided in ref 61.

AUTHOR INFORMATION

Corresponding Author

*E-mail: xavier.blase@neel.cnrs.fr.

Notes

The authors declare no competing financial interest.

ACKNOWLEDGMENTS

The authors are indebted to Jérôme Cornil for pointing out the reference to Alexander Mityashin's thesis and for a critical reading of the manuscript and thank Valerio Olevano for numerous discussions concerning the *GW* formalism applied to organic crystals. This project has received funding from the European Union Horizon 2020 research and innovation programme under Grant Agreement No. 646176 (EXTMOS) and No. 676629 (EoCoE). G.D. gratefully thanks Zoltán G. Soos for discussions on polarizable models and photoelectron spectroscopy and acknowledges support from EU through the FP7-PEOPLE-2013-IEF program (GA 2013-625198). D.B. is FNRS research director. This research used resources from the GENCI French national supercomputing resources.

DOI: 10.1021/acs.jpclett.6b01302
J. Phys. Chem. Lett. 2016, 7, 2814−2820

REFERENCES

(1) Warshel, A.; Levitt, M. Theoretical Studies of Enzymic Reactions: Dielectric, Electrostatic and Steric Stabilization of the Carbonium Ion in the Reaction of Lysozyme. *J. Mol. Biol.* **1976**, *103*, 227−249.

(2) Field, M. J.; Bash, P. A.; Karplus, M. A Combined Quantum Mechanical and Molecular Mechanical Potential for Molecular Dynamics Simulations. *J. Comput. Chem.* **1990**, *11*, 700−733.

(3) Norton, J. E.; Brédas, J.-L. Polarization Energies in Oligoacene Semiconductor Crystals. *J. Am. Chem. Soc.* **2008**, *130*, 12377−12384.

(4) Difley, S.; Wang, L.-P.; Yeganeh, S.; Yost, S. R.; Voorhis, T. V. Electronic Properties of Disordered Organic Semiconductors via QM/MM Simulations. *Acc. Chem. Res.* **2010**, *43*, 995−1004.

(5) Yost, S. R.; Wang, L.-P.; Van Voorhis, T. Molecular Insight Into the Energy Levels at the Organic Donor/Acceptor Interface: A Quantum Mechanics/Molecular Mechanics Study. *J. Phys. Chem. C* **2011**, *115*, 14431−14436.

(6) Friederich, P.; Symalla, F.; Meded, V.; Neumann, T.; Wenzel, W. Ab Initio Treatment of Disorder Effects in Amorphous Organic Materials: Toward Parameter Free Materials Simulation. *J. Chem. Theory Comput.* **2014**, *10*, 3720−3725.

(7) Hedin, L. New Method for Calculating the One-Particle Green's Function with Application to the Electron-Gas Problem. *Phys. Rev. A* **1965**, *139*, 796−823.

(8) Hybertsen, M. S.; Louie, S. G. Electron Correlation in Semiconductors and Insulators: Band Gaps and Quasiparticle Energies. *Phys. Rev. B: Condens. Matter Mater. Phys.* **1986**, *34*, 5390−5413.

(9) Godby, R. W.; Schlüter, M.; Sham, L. J. Self-Energy Operators and Exchange-Correlation Potentials in Semiconductors. *Phys. Rev. B: Condens. Matter Mater. Phys.* **1988**, *37*, 10159−10175.

(10) Onida, G.; Reining, L.; Rubio, A. Electronic Excitations: Density-Functional versus Many-Body Green's Function Approaches. *Rev. Mod. Phys.* **2002**, *74*, 601−659.

(11) Faber, C.; Attaccalite, C.; Olevano, V.; Runge, E.; Blase, X. First-Principles *GW* Calculations for DNA and RNA Nucleobases. *Phys. Rev. B: Condens. Matter Mater. Phys.* **2011**, *83*, 115123.

(12) Kaplan, F.; Weigend, F.; Evers, F.; van Setten, M. J. Off-Diagonal Self-Energy Terms and Partially Self-Consistency in *GW* Calculations for Single Molecules: Efficient Implementation and Quantitative Effects on Ionization Potentials. *J. Chem. Theory Comput.* **2015**, *11*, 5152−5160.

(13) Knight, J. W.; Wang, X.; Gallandi, L.; Dolgounitcheva, O.; Ren, X.; Ortiz, J. V.; Rinke, P.; Körzdörfer, T.; Marom, N. Accurate Ionization Potentials and Electron Affinities of Acceptor Molecules III: A Benchmark of *GW* Methods. *J. Chem. Theory Comput.* **2016**, *12*, 615−626.

(14) Kaplan, F.; Harding, M. E.; Seiler, C.; Weigend, F.; Evers, F.; van Setten, M. J. Quasi-Particle Self-Consistent *GW* for Molecules. *J. Chem. Theory Comput.* **2016**, *12*, 2528−2541.

(15) Rangel, T.; Hamed, S. M.; Bruneval, F.; Neaton, J. B. Evaluating the *GW* Approximation with CCSD(T) for Charged Excitations Across the Oligoacenes. *J. Chem. Theory Comput.* **2016**, *12*, 2834−2842.

(16) Tiago, M. L.; Kent, P. R. C.; Hood, R. Q.; Reboredo, F. A. Neutral and Charged Excitations in Carbon Fullerenes from First-Principles Many-Body Theories. *J. Chem. Phys.* **2008**, *129*, 084311.

(17) Palummo, M.; Hogan, C.; Sottile, F.; Bagalá, P.; Rubio, A. *Ab Initio* Electronic and Optical Spectra of Free-Base Porphyrins: The Role of Electronic Correlation. *J. Chem. Phys.* **2009**, *131*, 084102.

(18) Umari, P.; Stenuit, G.; Baroni, S. *GW* Quasiparticle Spectra from Occupied States Only. *Phys. Rev. B: Condens. Matter Mater. Phys.* **2010**, *81*, 115104.

(19) Rostgaard, C.; Jacobsen, K. W.; Thygesen, K. S. Fully Self-Consistent *GW* Calculations for Molecules. *Phys. Rev. B: Condens. Matter Mater. Phys.* **2010**, *81*, 085103.

(20) Blase, X.; Attaccalite, C.; Olevano, V. First-Principles *GW* Calculations for Fullerenes, Porphyrins, Phtalocyanine, and other Molecules of Interest for Organic Photovoltaic Applications. *Phys. Rev. B: Condens. Matter Mater. Phys.* **2011**, *83*, 115103.

(21) Foerster, D.; Koval, P.; Sánchez-Portal, D. An $O(N^3)$ Implementation of Hedin's *GW* Approximation for Molecules. *J. Chem. Phys.* **2011**, *135*, 074105.

(22) Marom, N.; Ren, X.; Moussa, J. E.; Chelikowsky, J. R.; Kronik, L. Electronic Structure of Copper Phthalocyanine from G_0W_0 Calculations. *Phys. Rev. B: Condens. Matter Mater. Phys.* **2011**, *84*, 195143.

(23) Baumeier, B.; Andrienko, D.; Rohlfing, M. Frenkel and Charge-Transfer Excitations in Donor-acceptor Complexes from Many-Body Greens Functions Theory. *J. Chem. Theory Comput.* **2012**, *8*, 2790−2795.

(24) Baumeier, B.; Andrienko, D.; Ma, Y.; Rohlfing, M. Excited States of Dicyanovinyl-Substituted Oligothiophenes from Many-Body Green's Functions Theory. *J. Chem. Theory Comput.* **2012**, *8*, 997−1002.

(25) Marom, N.; Caruso, F.; Ren, X.; Hofmann, O. T.; Körzdörfer, T.; Chelikowsky, J. R.; Rubio, A.; Scheffler, M.; Rinke, P. Benchmark of *GW* Methods for Azabenzenes. *Phys. Rev. B: Condens. Matter Mater. Phys.* **2012**, *86*, 245127.

(26) Caruso, F.; Rinke, P.; Ren, X.; Rubio, A.; Scheffler, M. Self-Consistent *GW*: All-Electron Implementation with Localized Basis Functions. *Phys. Rev. B: Condens. Matter Mater. Phys.* **2013**, *88*, 075105.

(27) Bruneval, F.; Marques, M. A. L. Benchmarking the Starting Points of the *GW* Approximation for Molecules. *J. Chem. Theory Comput.* **2013**, *9*, 324−329.

(28) Pham, T. A.; Nguyen, H.-V.; Rocca, D.; Galli, G. *GW* Calculations using the Spectral Decomposition of the Dielectric Matrix: Verification, Validation, and Comparison of Methods. *Phys. Rev. B: Condens. Matter Mater. Phys.* **2013**, *87*, 155148.

(29) Umari, P.; Giacomazzi, L.; De Angelis, F.; Pastore, M.; Baroni, S. Energy-Level Alignment in Organic Dye-Sensitized TiO_2 from *GW* Calculations. *J. Chem. Phys.* **2013**, *139*, 014709.

(30) Qian, X.; Umari, P.; Marzari, N. Photoelectron Properties of DNA and RNA Bases from Many-Body Perturbation Theory. *Phys. Rev. B: Condens. Matter Mater. Phys.* **2011**, *84*, 075103.

(31) Körbel, S.; Boulanger, P.; Duchemin, I.; Blase, X.; Marques, M. A. L.; Botti, S. Benchmark Many-Body *GW* and Bethe-Salpeter Calculations for Small Transition Metal Molecules. *J. Chem. Theory Comput.* **2014**, *10*, 3934−3943.

(32) Lischner, J.; Sharifzadeh, S.; Deslippe, J.; Neaton, J. B.; Louie, S. G. Effects of Self-Consistency and Plasmon-Pole Models on *GW* Calculations for Closed-Shell Molecules. *Phys. Rev. B: Condens. Matter Mater. Phys.* **2014**, *90*, 115130.

(33) Laflamme Janssen, J.; Rousseau, B.; Côté, M. Efficient Dielectric Matrix Calculations using the Lanczos Algorithm for Fast Many-Body G_0W_0 Implementations. *Phys. Rev. B: Condens. Matter Mater. Phys.* **2015**, *91*, 125120.

(34) Duchemin, I.; Deutsch, T.; Blase, X. Short-Range to Long-Range Charge-Transfer Excitations in the Zincbacteriochlorin-Bacteriochlorin Complex: A Bethe-Salpeter Study. *Phys. Rev. Lett.* **2012**, *109*, 167801.

(35) Baumeier, B.; Rohlfing, M.; Andrienko, D. Electronic Excitations in Push-Pull Oligomers and Their Complexes with Fullerene from Many-Body Green's Functions Theory with Polarizable Embedding. *J. Chem. Theory Comput.* **2014**, *10*, 3104−3110.

(36) Niedzialek, D.; Duchemin, I.; de Queiroz, T. B.; Osella, S.; Rao, A.; Friend, R.; Blase, X.; Kümmel, S.; Beljonne, D. First Principles Calculations of Charge Transfer Excitations in Polymer-Fullerene Complexes: Influence of Excess Energy. *Adv. Funct. Mater.* **2015**, *25*, 1972−1984.

(37) Govoni, M.; Galli, G. Large Scale *GW* Calculations. *J. Chem. Theory Comput.* **2015**, *11*, 2680−2696.

(38) Tiago, M. L.; Northrup, J. E.; Louie, S. G. *Ab Initio* Calculation of the Electronic and Optical Properties of Solid Pentacene. *Phys. Rev. B: Condens. Matter Mater. Phys.* **2003**, *67*, 115212.

(39) Sharifzadeh, S.; Biller, A.; Kronik, L.; Neaton, J. B. Quasiparticle and Optical Spectroscopy of the Organic Semiconductors Pentacene and PTCDA from First Principles. *Phys. Rev. B: Condens. Matter Mater. Phys.* **2012**, *85*, 125307.

DOI: 10.1021/acs.jpclett.6b01302
J. Phys. Chem. Lett. 2016, 7, 2814−2820

(40) Kang, Y.; Jeon, S. H.; Cho, Y.; Han, S. *Ab Initio* Calculation of Ionization Potential and Electron Affinity in Solid-State Organic Semiconductors. *Phys. Rev. B: Condens. Matter Mater. Phys.* **2016**, *93*, 035131.
(41) Rangel, T.; Berland, K.; Sharifzadeh, S.; Brown-Altvater, F.; Lee, K.; Hyldgaard, P.; Kronik, L.; Neaton, J. B. Structural and Excited-State Properties of Oligoacene Crystals from First Principles. *Phys. Rev. B: Condens. Matter Mater. Phys.* **2016**, *93*, 115206.
(42) Duchemin, I.; Jacquemin, D.; Blase, X. Combining the *GW* Formalism with the Polarizable Continuum Model: A State-Specific Non-Equilibrium Approach. *J. Chem. Phys.* **2016**, *144*, 164106.
(43) D'Avino, G.; Mothy, S.; Muccioli, L.; Zannoni, C.; Wang, L.; Cornil, J.; Beljonne, D.; Castet, F. Energetics of Electron-Hole Separation at P3HT/PCBM Heterojunctions. *J. Phys. Chem. C* **2013**, *117*, 12981−12990.
(44) D'Avino, G.; Muccioli, L.; Zannoni, C.; Beljonne, D.; Soos, Z. G. Electronic Polarization in Organic Crystals: A Comparative Study of Induced Dipoles and Intramolecular Charge Redistribution Schemes. *J. Chem. Theory Comput.* **2014**, *10*, 4959−4971.
(45) Perdew, J. P.; Ernzerhof, M.; Burke, K. Rationale for Mixing Exact Exchange with Density Functional Approximations. *J. Chem. Phys.* **1996**, *105*, 9982−9985.
(46) Adamo, C.; Barone, V. Toward Reliable Density Functional Methods without Adjustable Parameters: The PBE0Model. *J. Chem. Phys.* **1999**, *110*, 6158−6170.
(47) Dressel, M.; Gompf, B.; Faltermeier, D.; Tripathi, A.; Pflaum, J.; Schubert, M. Kramers-Kronig-Consistent Optical Functions of Anisotropic Crystals: Generalized Spectroscopic Ellipsometry on Pentacene. *Opt. Express* **2008**, *16*, 19770.
(48) Bruneval, F.; Vast, N.; Reining, L. Effect of Self-Consistency on Quasiparticles in Solids. *Phys. Rev. B: Condens. Matter Mater. Phys.* **2006**, *74*, 045102.
(49) Neaton, J. B.; Hybertsen, M. S.; Louie, S. G. Renormalization of Molecular Electronic Levels at Metal-Molecule Interfaces. *Phys. Rev. Lett.* **2006**, *97*, 216405.
(50) Garcia-Lastra, J. M.; Thygesen, K. S. Renormalization of Optical Excitations in Molecules near a Metal Surface. *Phys. Rev. Lett.* **2011**, *106*, 187402.
(51) Blase, X.; Attaccalite, C. Charge-Transfer Excitations in Molecular Donor-Acceptor Complexes within the Many-Body Bethe-Salpeter Approach. *Appl. Phys. Lett.* **2011**, *99*, 171909.
(52) Weigend, F. Accurate Coulomb-Fitting Basis Sets for H to Rn. *Phys. Chem. Chem. Phys.* **2006**, *8*, 1057−1065.
(53) Tsiper, E. V.; Soos, Z. G. Charge Redistribution and Polarization Energy of Organic Molecular Crystals. *Phys. Rev. B: Condens. Matter Mater. Phys.* **2001**, *64*, 195124.
(54) Soos, Z.; Tsiper, E. V.; Pascal, R. Charge Redistribution and Electronic Polarization in Organic Molecular Crystals. *Chem. Phys. Lett.* **2001**, *342*, 652−658.
(55) D'Avino, G.; Vanzo, D.; Soos, Z. G. Dielectric Properties of Crystalline Organic Molecular Films in the Limit of Zero Overlap. *J. Chem. Phys.* **2016**, *144*, 034702.
(56) Bounds, P. J.; Munn, R. W. Polarization Energy of a Localized Charge in a Molecular Crystal. II. Charge-Quadrupole Energy. *Chem. Phys.* **1981**, *59*, 41−45.
(57) Salzmann, I.; Duhm, S.; Heimel, G.; Oehzelt, M.; Kniprath, R.; Johnson, R. L.; Rabe, J. P.; Koch, N. Tuning the Ionization Energy of Organic Semiconductor Films: The Role of Intramolecular Polar Bonds. *J. Am. Chem. Soc.* **2008**, *130*, 12870−12871.
(58) Topham, B. J.; Soos, Z. G. Ionization in Organic Thin Films: Electrostatic Potential, Electronic Polarization, and Dopants in Pentacene Films. *Phys. Rev. B: Condens. Matter Mater. Phys.* **2011**, *84*, 165405.
(59) Yoshida, H.; Yamada, K.; Tsutsumi, J.; Sato, N. Complete Description of Ionization Energy and Electron Affinity in Organic Solids: Determining Contributions from Electronic Polarization, Energy Band Dispersion, and Molecular Orientation. *Phys. Rev. B: Condens. Matter Mater. Phys.* **2015**, *92*, 075145.
(60) Tsiper, E.; Soos, Z.; Gao, W.; Kahn, A. Electronic Polarization at Surfaces and Thin Films of Organic Molecular Crystals: PTCDA. *Chem. Phys. Lett.* **2002**, *360*, 47−52.
(61) Siegrist, T.; Kloc, C.; Schön, J. H.; Batlogg, B.; Haddon, R. C.; Berg, S.; Thomas, G. A. Enhanced Physical Properties in a Pentacene Polymorph. *Angew. Chem., Int. Ed.* **2001**, *40*, 1732−1736.
(62) Crocker, L.; Wang, T.; Kebarle, P. Electron Affinities of some Polycyclic Aromatic Hydrocarbons, Obtained from Electron-Transfer Equilibria. *J. Am. Chem. Soc.* **1993**, *115*, 7818−7822.
(63) Coropceanu, V.; Malagoli, M.; da Silva Filho, D. A.; Gruhn, N. E.; Bill, T. G.; Brédas, J. L. Hole- and Electron-Vibrational Couplings in Oligoacene Crystals: Intramolecular Contributions. *Phys. Rev. Lett.* **2002**, *89*, 275503.
(64) Campbell, R. B.; Robertson, J. M.; Trotter, J. The Crystal Structure of Hexacene, and a Revision of the Crystallographic Data for Tetracene. *Acta Crystallogr.* **1962**, *15*, 289−290.
(65) Schiefer, S.; Huth, M.; Dobrinevski, A.; Nickel, B. Determination of the Crystal Structure of Substrate-Induced Pentacene Polymorphs in Fiber Structured Thin Films. *J. Am. Chem. Soc.* **2007**, *129*, 10316−10317.
(66) The notation GW_0 indicates that only the Green's function *G* as been updated self-consistently.
(67) Zhao, Y.; Truhlar, D. G. The M06 Suite of Density Functionals for Main Group Thermochemistry, Thermochemical Kinetics, Noncovalent Interactions, Excited States, and Transition Elements: Two New Functionals and Systematic Testing of Four M06-Class Functionals and 12 Other Functionals. *Theor. Chem. Acc.* **2008**, *120*, 215−241.
(68) Gorczak, N.; Swart, M.; Grozema, F. C. Energetics of Charges in Organic Semiconductors and at Organic Donor-Acceptor Interfaces. *J. Mater. Chem. C* **2014**, *2*, 3467−3475.
(69) Castet, F.; Aurel, P.; Fritsch, A.; Ducasse, L.; Liotard, D.; Linares, M.; Cornil, J.; Beljonne, D. Electronic Polarization Effects on Charge Carriers in Anthracene: A Valence Bond Study. *Phys. Rev. B: Condens. Matter Mater. Phys.* **2008**, *77*, 115210.
(70) Ratcliff, L. E.; Grisanti, L.; Genovese, L.; Deutsch, T.; Neumann, T.; Danilov, D.; Wenzel, W.; Beljonne, D.; Cornil, J. Toward Fast and Accurate Evaluation of Charge On-Site Energies and Transfer Integrals in Supramolecular Architectures Using Linear Constrained Density Functional Theory (CDFT)-Based Methods. *J. Chem. Theory Comput.* **2015**, *11*, 2077−2086.
(71) Eilmes, A.; Munn, R. W. Microscopic Calculation of the Energetics of Charged States in Amorphous Polyethylene. *J. Chem. Phys.* **2004**, *120*, 7779−7783.
(72) Mityashin, A. Predictive Modelling of Organic Molecular Semiconductors. Ph.D. thesis, KU Leuven, 2013.
(73) D'Avino, G.; Olivier, Y.; Muccioli, L.; Beljonne, D. Do Charges Delocalize Over Multiple Molecules in Fullerene Derivatives? *J. Mater. Chem. C* **2016**, *4*, 3747−3756.
(74) D'Avino, G.; Muccioli, L.; Olivier, Y.; Beljonne, D. Charge Separation and Recombination at Polymer-Fullerene Heterojunctions: Delocalization and Hybridization Effects. *J. Phys. Chem. Lett.* **2016**, *7*, 536−540.
(75) Valiev, M.; Bylaska, E.; Govind, N.; Kowalski, K.; Straatsma, T.; Van Dam, H. J. J.; Wang, D.; Nieplocha, J.; Apra, E.; Windus, T.; et al. NWChem: A Comprehensive and Scalable Open-Source Solution for Large Scale Molecular Simulations. *Comput. Phys. Commun.* **2010**, *181*, 1477−1489.
(76) Dunning, T. H. Gaussian Basis Sets for Use in Correlated Molecular Calculations. I. The Atoms Boron through Neon and Hydrogen. *J. Chem. Phys.* **1989**, *90*, 1007−1023.
(77) Weigend, F.; Köhn, A.; Hättig, C. Efficient Use of the Correlation Consistent Basis Sets in Resolution of the Identity MP2 Calculations. *J. Chem. Phys.* **2002**, *116*, 3175−3183.
(78) Hickey, A. L.; Rowley, C. N. Benchmarking Quantum Chemical Methods for the Calculation of Molecular Dipole Moments and Polarizabilities. *J. Phys. Chem. A* **2014**, *118*, 3678−3687.

DOI: 10.1021/acs.jpclett.6b01302
J. Phys. Chem. Lett. 2016, 7, 2814−2820